Solution-Based Chemical Synthesis of Boehmite Nanofibers and Alumina Nanorods

Suresh C. Kuiry,† Ed Megen, Swanand D. Patil, Sameer A. Deshpande, and Sudipta Seal*

Surface Engineering and Nanotechnology Facility, Advanced Materials Processing and Analysis Center, University of Central Florida, 4000 Central Florida Boulevard, Eng. 1, #381, Orlando, Florida 32816

Received: September 21, 2004; In Final Form: December 22, 2004

This article reports an easy chemical method of synthesizing boehmite nanofibers by a modified sol−gel process involving aluminum isopropoxide precursor. Nanorods of γ-alumina have been successfully prepared after dehydration of the viscous sol at 600 °C for 4 h in air. The boehmite nanofibers and γ-alumina nanorods were characterized by X-ray photoelectron spectroscopy, Fourier transform infrared spectroscopy for surface chemistry and functional groups, scanning electron microscopy, high-resolution transmission electron microscopy with selected area electron diffraction, and energy-dispersed spectroscopy for morphology and structure identification. The length of the boehmite nanofibers was found to be more than 10 μm with a crystalline lattice structure. The mechanism of formation of the boehmite nanofibers included the preferential growth along the longitudinal axis due to interaction between the solvent molecules and the surface OH^- groups of hydrogen bonds. It is also suggested that the boehmite nanofibers may have formed due to the inherent instability of the planar structure of the boehmite lattice. The diameter of the γ-alumina nanorods was found to be less than 10 nm with a varying length in the range of 50−200 nm. Boehmite to γ-Al_2O_3 transformation was attributed to the loss of water molecules by internal condensation of protons and hydroxyl ions.

Introduction

Nanosized materials, especially one-dimensional nanomaterials such as nanowires, nanorods, and nanotubes, have great potential for nanodevice applications in nanoelectronics, photonics, data recording media, gas sensing, and gas storage.[1−3] Such one-dimensional systems offer new opportunities for investigating their size- and shape-dependent optical, magnetic, and electronic properties[4−6] with a possibility of embodying unique characteristics.[7] Numerous studies on the oxides of titanium, vanadium, zinc, silicon, and tungsten in the nanosize domain have been carried out for various applications such as improved catalytic behavior, nonlinear optical characteristics, and unusual luminescence properties. Nanosized materials provide a large surface area compared to their micro and macro counterparts. The quantum size effect[8] is well-known for semiconductor nanoparticles, which is revealed by a blue shift of absorption edge and photoluminescence. Barnakov et al.[9] reported a blue shift due to quantum confinement of exciton in the nanorodlike lead iodide crystallites of dimension 70 nm length and 10 nm diameter, which were synthesized by a microemulsion method in toluene medium with sodium dodecyl benzenesulfonate as surfactant and methanol as cosurfactant.

Shen et al.[10] synthesized nickel sulfide nanorods by a procedure that involved a reaction for a prolonged period of time in an autoclave maintained at 165 °C. Although the detailed mechanism of the formation of nanorods was not clear, it was suggested that such nanorods of sulfides formed due to a coordinated growth with S^{2-} at temperatures higher than 160 °C vis-à-vis instability of the Ni^{2+} complex with hydrazine. Hydrothermal growth of $La(OH)_3$ nanorods was studied by others.[11] Fan et al.[6] observed the formation of single-crystal nanorods, nanowires, and nanotubes of $Mg(OH)_2$ by a solvothermal process with the help of the solvent coordination molecular template. The type of nanostructure formed was found to be strongly influenced by the nature of solvents, their coordination ability, and the reaction temperature. To prepare nanorods of titanium dioxide, Miao et al.[7] employed a dip-coating process in which titania sol was produced from the sol−gel reaction of titanium tetraisopropoxide, ethanol, acetyl acetone, and water on anodic alumina membranes. Subsequently, by dissolving the alumina template structure in 10% aqueous H_3PO_4 solution at 50 °C, TiO_2 nanorods with a diameter of about 200 nm and length of several micrometers could be obtained. Synthesis of nanorods of titania on a glass surface through anodic oxidation of sputtered aluminum followed by sol−gel dip coating or electrodeposition has also been reported by others.[12]

Despite numerous studies utilizing various methods, as indicated above, on synthesis and characterization of hydroxide, oxide, and sulfide nanorods, a detailed investigation leading to the formation of alumina nanorods is not available to date. A preliminary study was reported by Khalil[13] on the synthesis of a fibrous boehmite [AlO(OH)]. However, the sol was not characterized[13] by any analytical tool. Alumina nanorods have excellent high temperature stability and can be extensively used for catalytic supports in gas−gas separation and petrochemical processing, especially during re-forming and isomerization.[14] In continuation of the tubular nanostructural research[15,16] from this laboratory and keeping in view such aspects of novel applications of alumina nanostructures, the present article reports the development of a process to synthesize boehmite nanofibers and their subsequent transformation to γ-alumina nanorods by a simplified and less cumbersome process.

* Corresponding author: phone 407-882-1119; e-mail sseal@mail.ucf.edu.
† Present address: Center for Tribology, Inc., 1715 Dell Ave., Campbell, CA 95008.

10.1021/jp045706k CCC: $30.25
Published on Web 02/09/2005

Experimental Section

One-dimensional nanorod/fiber synthesis was carried out by a modified sol−gel process. The conventional processes[17−19] for alumina synthesis utilize excess water for hydrolysis of the aluminum alkoxide at about 80 °C, followed by a series of synthesis steps such as peptization in mild acidic condition, solvent evaporation, drying, and calcination. The present modified sol−gel process for synthesis of boehmite fibers and γ-alumina nanorods, however, requires not only less water but also less intermediate steps. In the present process, a solution of 0.1 M aluminum isopropoxide was prepared in anhydrous ethanol by magnetic stirring. Another ethanol solution with 4% water was prepared that was added to the aluminum isopropoxide solution with continued stirring. The mixture was allowed to react for 15 h to form a viscous liquid. Transmission electron microscopy (TEM) specimen was prepared from the viscous liquid to study the shape and crystal structure of the resulted materials. The viscous substance was heated at 600 °C for 4 h in air. A powder residue was obtained. The powder was analyzed by scanning electron microscopy (SEM), X-ray photoelectron spectroscopy (XPS), and high-resolution transmission electron microscopy (HRTEM) for its particle morphology, chemistry, and shape and size distribution. A TEM specimen was prepared by dispersing the powder in absolute ethanol by ultrasonication.

The morphology of the alumina nanorods was characterized on a JEOL T-300 SEM system with accelerating voltage of 4 kV for imaging. HRTEM and scanning transmission electron microscopy coupled with energy dispersion spectroscopy studies were carried out, on a Philips 300 TECNAI at 300 kV, to investigate the elemental composition, size and structure of the alumina nanorods. Selected area electron diffraction (SAED) pattern of alumina nanorods was also collected from TEM studies. An XPS (Perkin-Elmer PHI 5400) study was carried out with Mg Kα X-rays of energy 1253.6 eV at a power of 250 W. Survey and individual high-resolution spectra were recorded with pass energies of 44.75 and 35.75 eV, respectively. The spectrometer was calibrated by use of a metallic gold standard [Au ($4f_{7/2}$) = 84.0 ± 0.1 eV]. Charging shifts were removed by use of a binding energy of C (1s) of the adventitious carbon[20] at 284.6 eV.

Fourier transform infrared (FTIR) spectroscopy was utilized to characterize the alumina nanorods on a Perkin-Elmer Spectrum One FT-IR with attenuated total reflectance (ATR) accessories. The transmittance data were recorded and analyzed with the software Spectrum One B, v 5.0, on a computer with a Pentium processor that was connected to the FTIR equipment.

Results and Discussion

Figure 1 shows a TEM image of nanorods observed from the viscous specimen formed after hydrolysis and condensation with aluminum isopropoxide and ethanol. The diameter of the nanorods varies, as evidenced from Figure 1; however, the length of some of the rods was more than 10 μm. Figure 2 depicts a HRTEM image of a portion of a long alumina nanorod with a diameter of about 120 nm. The surface of the nanorod exhibits a wavy pattern, probably due to the uneven volume changes during the room-temperature drying of the sol at the time of specimen preparation on a TEM grid. Figure 3 is the EDS spectrum of the nanorods obtained during the TEM study, which revealed the presence of both aluminum and oxygen. A copper grid was used in the TEM study; therefore, Figure 3 revealed a Cu signal in the spectrum. The SAED pattern obtained from the alumina nanorods specimen is presented in Figure 4. After indexing of the SAED pattern, it was found

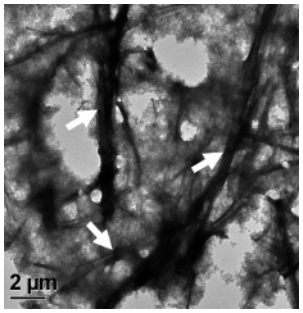

Figure 1. TEM image of boehmite nanofibers. Some are shown with arrows, observed from the viscous specimen formed after hydrolysis and condensation with aluminum isopropoxide, ethanol, and water.

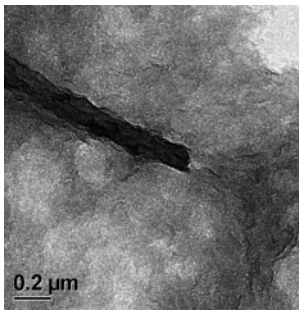

Figure 2. HRTEM image of a boehmite nanofiber observed in the viscous specimen formed after hydrolysis and condensation with aluminum isopropoxide, ethanol, and water.

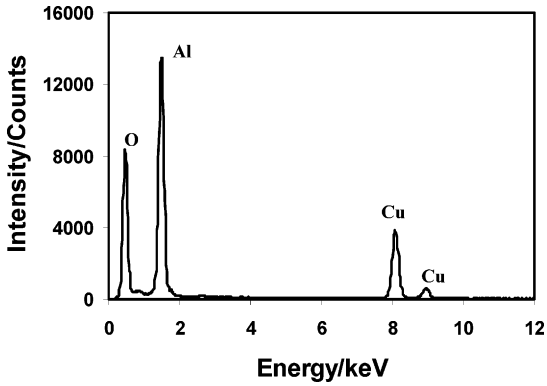

Figure 3. EDS spectrum of boehmite nanorods as shown in Figure 1, obtained from TEM investigation showing the presence of Al and oxygen; Cu signal was from the TEM grid.

that the crystal structure of the nanorods was of boehmite phase with orthorhombic crystal structure, which matches well with the data available in the JCPDS powder diffraction file 21-1307. It is interesting to note that Popa et al.[21] observed similar diffraction pattern on a boehmite film that was obtained with the help of a different sol−gel method.[17] These films were not investigated by TEM to reveal the shape of the crystalline boehmite phase. Therefore, it was not clear from their study[21] about the morphology and structure of the boehmite phase. Although boehmite exhibits excellent crystallinity, which was confirmed by XRD studies, it was reported[22] that water intercalation took place in the presence of excess water, causing swelling and subsequent loss of crystallinity. Such a structure of the boehmite was termed superamorphous. In the present study, however, the formation of superamorphous boehmite phase was not observed because the water content in the process was restricted.

Mechanism of Boehmite Nanorod Formation. The formation of boehmite [AlO(OH)] in the present investigation can be

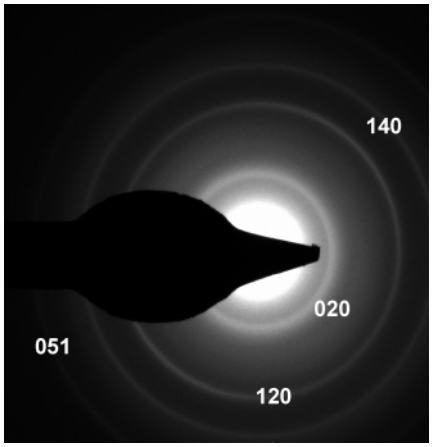

Figure 4. SAED pattern obtained from boehmite nanofibers presented in Figure 1, confirming the presence of a crystalline boehmite phase.

envisaged by the following hydrolysis and alcohol condensation reaction:

$$(CH_3CH_2CH_2O)_3Al + 2H_2O = AlO(OH) + 3CH_3CH_2CH_2OH \quad (1)$$

Such a hydrolysis reaction of metal alkoxide is common in the sol−gel process for synthesis of ceramic particulates.[19] Since there was no precipitation during the synthesis, it is likely that the hydrolysis reaction was incomplete and possibly parallel polymerization reactions led to the formation of the rodlike nanostructure of Al-oxy-hydroxide. It should be mentioned that the water content in the present method of synthesis was also less; therefore, partial hydrolysis and subsequent condensation of such species is the most likely process one can envisage. Partial hydrolysis due to the limited water content in the system is more likely to retain the original oligomeric structure. The condensation process between partially hydrolyzed species with retained oligomeric structure has possibly helped in producing nanofibrous structure in the present situation. Such a mechanism of formation of fibrous boehmite has also been suggested by others.[18,22] According to Pierre and Uhlmann,[22] oxygen ions are arranged in a distorted octahedral configuration around aluminum in the boehmite lattice and are organized in a parallel layers linked by hydrogen bonds. Each layer of octahedral configuration has two sublayers. Popa et al.[21] suggested that the Al atoms in the boehmite lattice form a deformed octahedron with four oxygen and two hydroxide neighbors. Such octahedra joined by edges result in AlO(OH) polymeric layers. These layers are held together by hydrogen bonds between the OH^- groups of each octahedron. Figure 5 depicts a schematic diagram exhibiting the organization of Al and oxygen atoms along with hydrogen bonding between two adjacent layers.

Boehmite has a preferential growth direction due to the presence of weak hydrogen bonds and interaction between the solvent molecules and the surface OH^- groups via hydrogen bonds. Perhaps such interaction led to the formation of the tubular nanostructure of the boehmite during sol−gel processing in the present investigation as shown in Figures 1 and 2. Such a solvent-molecule-coordinated preferential growth mechanism leading to the formation of nanorods of other metal hydroxide systems was reported by previous workers.[6,11] Although the exact mechanism of the formation of such nanostructure morphology remained elusive, the preferential and directional growth to form such structure might be influenced by several factors such as nature of the crystal structure, coordination

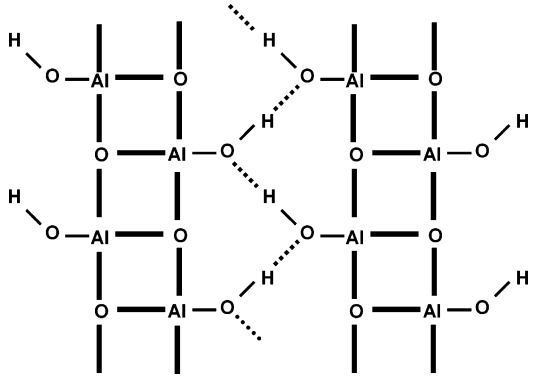

Figure 5. Schematic representation of a portion of planar boehmite lattice structure: two layers are held together by hydrogen bonds shown with dotted lines.

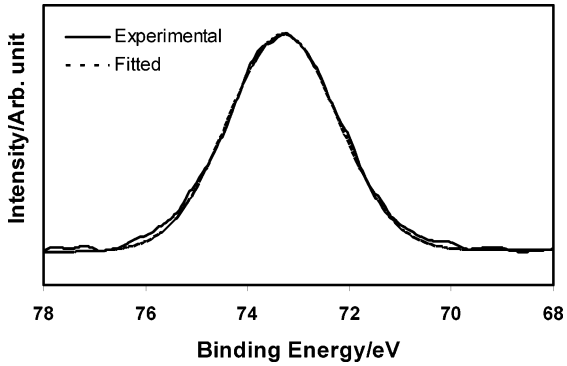

Figure 6. Peak-fitted XPS Al(2p) spectrum of nanorods obtained after thermal treatment of the viscous boehmite nanofiber sol at 600 °C for 4 h, confirming the formation of γ-alumina nanorods.

chemistry, reaction kinetics, and thermodynamics. The manifestation of tubular morphology possibly yields minimum free energy through optimization of configurational entropy under the present circumstances.

It might also happen that the planar boehmite layer was unstable beyond a certain size along the length and the breadth in the present case; a group of such sheets of critical dimensions possibly curled up and eventually joined edge-to-edge with the help of hydrogen bonds between hydrogen from hydroxyl group and the oxygen link between two Al atoms, as shown in Figure 5. Although a comparative study on the thermodynamic stability of the nanorod-shaped over the layered structure of boehmite is not available, extensive theoretical investigation[23] on graphene sheet revealed that tubular structure is energetically more stable than a flat sheetlike structure. Although generalization of such behavior may not be applicable in all systems, the confirmation of higher stability of boehmite fiber than that of a planar morphology definitely needs further theoretical study.

Transformation Mechanism of Boehmite to Form γ-Alumina Nanorods. XPS Al(2p) and O(1s) spectra of the nanorods obtained after heating of the sol at 600 °C in air are presented in Figures 6 and 7, respectively. The binding energy values along with full width at half-maximum (fwhm) of Al(2p) and O(1s) peaks observed in the present study, and those values available in the literature for γ-Al_2O_3, are presented in Table 1.

A recent XPS study[27] on the aluminum oxide formed on an alloy substrate revealed similar binding energy values for Al(2p) and O(1s) peaks. Such binding energy values and the presence of a much wider fwhm in the XPS Al(2p) spectrum in the present study further confirm that the nanorods consisted of γ-Al_2O_3. After carrying out detailed experimental and theoretical investigations, previous researchers[25] have suggested that va-

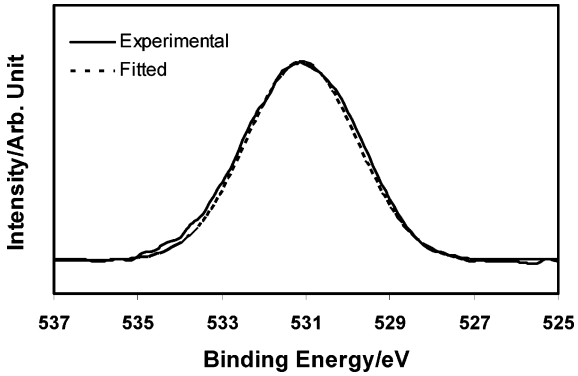

Figure 7. Peak-fitted XPS O(1s) spectrum of nanorods obtained after thermal treatment of the viscous boehmite nanofiber sol at 600 °C for 4 h confirming the formation of γ-alumina nanorods.

TABLE 1: XPS Binding Energy and Full Width at Half-Maximum Values for Al(2p) and O(1s) Peaks from γ-Al_2O_3

	Al(2p)/eV	fwhm/eV	O(1s)/eV	fwhm/eV
present study	73.5	2.4	531.1	2.8
Wagner et al.[24]	73.7		530.9	
Thomas and Sherwood[25]	74.2	2.2	530.5	2.9
Barr et al.[26]	73.9		530.6	

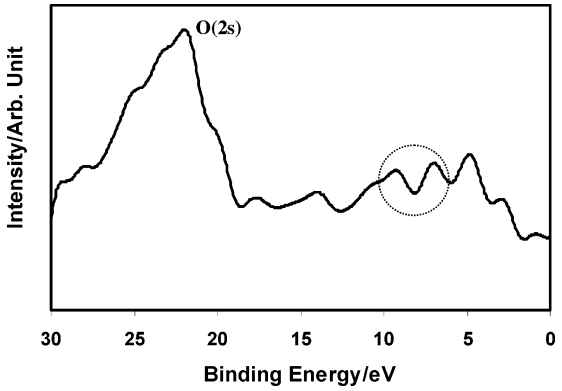

Figure 8. XPS valence band region of γ-alumina nanorods.

lence band spectrum can exhibit distinct features, which can be used successfully to identify certain oxide compounds. An XPS valence band spectrum of the nanorods is shown in Figure 8, which contains a number of features. For example, an intense peak, centered at the binding energy value of 22.3 eV, could be observed in Figure 8, which is identified to be due to O(2s). Among various other peaks, a band of peaks positioned at the binding energy range of 10 and 5 eV are noteworthy. These peaks are encircled in Figure 8 for easy identification. Similar valence band spectra were also observed by others for microcrystalline[25] and nanocrystalline[28] γ-alumina. The presence of such peaks in the valence band spectrum confirms that the nanorods in the present case comprise a γ-Al_2O_3 phase.

Figure 9 reveals the HRTEM image of the alumina nanorods powder obtained from the sol, which confirmed the presence of nanorods. However, the size of such nanostructures was definitely different from that observed on the sol specimens as shown in Figures 1 and 2. The diameter of the nanorods was less than 10 nm and the length varies from 50 to 200 nm. Figure 10 shows the SAED pattern taken from the nanorods during TEM investigation. The alumina nanorods formed after thermal treatment of the sol were found to be crystalline as indicated by the presence of rings in Figure 10. The closest match of the ring pattern was found to be that of γ-alumina with cubic structure (JCPDS file 10-425) out of numerous metastable

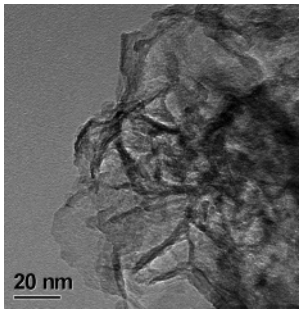

Figure 9. HRTEM image of γ-alumina nanorods after heating of the boehmite nanofiber sol at 600 °C for 4 h.

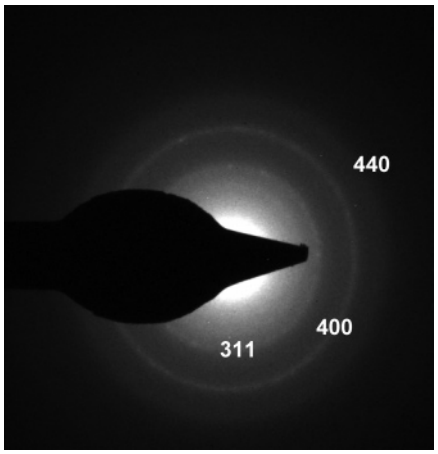

Figure 10. SAED pattern of γ-alumina nanorod obtained after heating of the boehmite nanofiber sol at 600 °C for 4 h.

phases of transition aluminum oxides[29,30] such as η, γ, χ, δ, κ, θ, and α. The evolution of the XRD pattern during the dehydration of boehmite phases has been reported recently by Krokidis et al.[14] on the basis of an elaborate theoretical investigation. The diffracting planes corresponding to the ring pattern in the present study matches excellently well with the simulated pattern of alumina after complete transformation of boehmite as reported by them.[14] The thermal treatment of boehmite at 600 °C for 4 h leads to the dehydration of physically adsorbed, structural, and intercalated water,[13] transforming the boehmite into γ-alumina. Such a transformation usually takes place by removal of one water molecule from two AlO(OH) octahedra with the help of an internal condensation of a proton and a hydroxyl ion. The oxygen ion serves as an anion link between two Al atoms, which belong to two adjacent boehmite lattices, retaining the overall original rod shape. Such a condensation process and removal of water molecule can be easily visualized from the schematic representation in Figure 5. According to Wilson and Stacey,[31] rearrangement of the oxygen atoms takes place during such a topotactic transformation of boehmite into γ-alumina. Interestingly, the rod morphology of the original boehmite phase was retained after the transformation on heating in the present investigation, as shown in Figure 9. Nevertheless, the size of the alumina nanofibers was found to be reduced in diameter and length, giving them a more nanorod morphology after thermal treatment at 600 °C for 4 h. This was possibly due to the structural rearrangement and partial collapse of the boehmite lattice during dehydration process. Perhaps the original boehmite fibers disintegrated at some locations along the length, forming shorter nanorods of γ-alumina. Soled[32] reported that γ-alumina has a hydroxylated surface, and upon heating at temperatures above 200 °C, surface hydroxyls groups were lost, which was followed by incorpora-

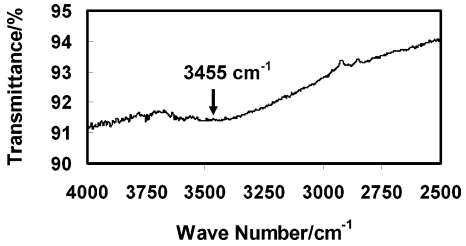

Figure 11. FT-IR spectra of γ-alumina nanorods obtained after heating of the viscous boehmite nanofiber sol at 600 °C for 4 h.

tion of terminal oxide ions that bridge two units. Such anion bridging with the help of surface hydroxylated ions and subsequent transformation of boehmite into γ-alumina invariably leads to particle growth. However, the present TEM study revealed that there was no growth of particles during the dehydration process of boehmite fibers and their subsequent formation of γ-alumina nanorods. Therefore, in the present situation, such bridging probably took place in the boehmite fiber structure itself without involving any other adjacent fiber. Hence, there was no indication of particle growth. It can be mentioned that XPS investigation did not reveal the presence of OH^- groups on the surface of the nanorods after heating. The XPS O(1s) envelope (Figure 7) revealed a symmetric peak for γ-Al_2O_3. Wang et al.[29] observed an intense absorption edge at wavenumber 3455 cm^{-1}, corresponding to the hydroxyls on the boehmite surface; the OH^- groups were present on the surface of γ-alumina even after heating at 800 °C for 8 h, which was probably attributed to the use of a large quantity of water. To probe such observations, an FTIR study was conducted on the alumina nanorod specimen. Figure 11 shows an FTIR spectrum of γ-alumina nanorods. Interestingly, unlike previous results,[29] the absorption edge of the hydroxyl group was found to be absent in the γ-alumina nanorods prepared in the present process, as evidenced from the FTIR spectrum in Figure 11, which further supports the trend of results of present XPS investigation. The boehmite to γ-alumina nanorods transformation was possibly attributed to the loss of water molecules by internal condensation of protons and hydroxyl ions. The initial stage of the dehydration process forming γ-alumina in the present investigation can be presented by the following equation:

$$2n\mathrm{AlO(OH)} \xrightarrow[-n\mathrm{H_2O}]{\text{heating}} n(\mathrm{Al_{2-\delta}O_3}) \qquad (2)$$

where δ is the extent of nonstoichiometry in terms of vacancy in the Al sublattice. When the dehydration is complete, all Al atoms occupy octahedral sites and a network of cation vacancies exists locally in the interlayer spaces.[14] However, at the final stage of the transformation, the migration of such cationic defects took place with the help of thermal energy and a more uniform distribution of defects in the structure took place. Formation of such defects in the γ-alumina lattice was also confirmed by Wang et al.[29] using nuclear magnetic resonance techniques. Disintegration of the original boehmite nanofibers into smaller fragments at certain locations during the dehydration process was possibly attributed to the presence of an array of such cation vacancies at those locations, eventually forming γ-alumina nanorods in the present study.

Conclusions

1. Synthesis of boehmite nanofibers by a modified sol−gel process with aluminum isopropoxide precursor at room temperature is feasible. Although the diameter varies, the length of the boehmite nanofibers was found to be more than 10 μm. Selected area electron diffraction study revealed the crystalline nature of the boehmite nanofibers.

2. The mechanism of the boehmite nanofiber formation was possibly due to preferential growth along the longitudinal direction, partly due to the interaction of the solvent molecules and the surface OH^- groups via hydrogen bonds and partly due to the inherent instability of the planar structure of the boehmite lattice.

3. Thermal treatment of the boehmite nanofibers at 600 °C for 4 h in air yields γ-Al_2O_3 nanorods. The diameter of the nanorods was less than 10 nm with a varying length in the range of 50−200 nm.

4. Boehmite to γ-Al_2O_3 transformation was attributed to the loss of water molecules by internal condensation of protons and hydroxyl ions.

Acknowledgment. We thank the NSF-REU programs (EEC 0139614 for funding E.M., a REU student, and EEC 0136710) and ONR Young Investigator Award N000140210591 for financial support of this nanoresearch.

References and Notes

(1) Snoke, D. *Science* **1996**, *273*, 1351.
(2) Rao, A. M.; Richter, E.; Bandow, S.; Shase, B.; Eklund, P. C.; Williams, L. A.; Fang, S.; Subbaswamy, K. R.; Menon, M.; Thess, A.; Smalley, R. E.; Dresselhaus, G.; Dresselhaus, M. S. *Science* **1997**, *275*, 187.
(3) Mirkin, C. A. *Science* **1999**, *286*, 2095.
(4) Alivisatos, A. P. *Science* **1996**, *271*, 933.
(5) Lieber, C. M. *Solid State Commun.* **1998**, *107*, 607.
(6) Fan, W.; Sun, S.; Song, X.; Zhang, W.; Yu, H.; Tan, X.; Cao, G. *J. Solid State Chem.* **2004**, *177*, 2329.
(7) Miao, L.; Tanemura, S.; Toh, S.; Kaneko, K.; Tanemura, M. *J. Crystal Growth* **2004**, *264*, 246.
(8) Stucky, G. D.; MacDougall, J. E. *Science* **1990**, *247*, 669.
(9) Barnakov, Yu. A.; Ito, S.; Dmitruk, I.; Tsunekawa, S.; Kasuya, A. *Scr. Mater.* **2001**, *45*, 273.
(10) Shen, G.; Chen, D.; Tang, K.; An, C.; Yang, Q.; Qian, Y. *J. Solid State Chem.* **2003**, *173*, 227.
(11) Deng, Y.; Wu, J.; Liu, J.; Wei, G. D.; Nan, C. W. *J. Phys. Chem. Solids* **2003**, *64*, 607.
(12) Inoue, S.; Chu, S.-Z.; Wada, K.; Li, D.; Haneda, H. *Sci. Technol. Adv. Mater.* **2003**, *4*, 269.
(13) Khalil, K. M. S. *J. Catal.* **1998**, *178*, 198.
(14) Krokidis, X.; Raybaud, P.; Gobichon, A.-E.; Rebours, B.; Euzen, P.; Toulhoat, H. *J. Phys. Chem. B* **2001**, *105*, 5121.
(15) Bera, D.; Kuiry, S. C.; McCutchen, M.; Kruize, A.; Heinrich, H.; Meyyappan, M.; Seal, S. *Chem. Phys. Lett.* **2001**, *386*, 364.
(16) Bera, D.; Kuiry, S. C.; McCutchen, M.; Seal, S.; Heinrich, H.; Slane, G. C. *J. Appl. Phys.* **2004**, *96*, 5152.
(17) Yoldas, B. E. *J. Mater. Sci.* **1975**, *10*, 1856.
(18) Assih, T.; Ayral, A.; Abenoza, M.; Phalippou, J. *J. Mater. Sci.* **1988**, *23*, 3326.
(19) Brinker, C. J.; Scherer, G. W. *Sol−Gel Science−The Physics and Chemistry of Sol−Gel Processing*; Academic Press: San Diego, CA, 1989; p 863.
(20) Barr, T. L.; Seal, S. *J. Vac. Sci. Technol.* **1995**, *A13*, 1239.
(21) Popa, A. F.; Rossignol, S.; Kappenstein, C. *J. Non-Cryst. Solids* **2002**, *306*, 169.
(22) Pierre, A. C.; Uhlmann, D. R. *J. Non-Cryst. Solids* **1986**, *82*, 271.
(23) Sawada, S.; Hamada, N. *Solid State Commun.* **1992**, *83*, 917.
(24) Wagner, C. D.; Passoja, D. E.; Hillery, H. F.; Kinisky, T. G.; Six, H. A.; Jansen, W. T.; Taylor, J. A. *J. Vac. Sci. Technol.* **1982**, *21*, 933.
(25) Thomas, S.; Sherwood, P. M. A. *Anal. Chem.* **1992**, *64*, 2488.
(26) Barr, T. L.; Seal, S.; Wozniak, K.; Klinowski, J. *J. Chem. Soc., Faraday Trans.* **1997**, *93*, 181.
(27) Kuiry, S. C.; Seal, S.; Fei, W.; Quick, N. *Oxid. Metals* **2003**, *59*, 543.
(28) Moffitt, C. E.; Chen, B.; Wieliczka, D. M.; Kruger, M. B. *Solid State Commun.* **2000**, *116*, 631.
(29) Wang, J. A.; Bokhimi, X.; Morales, A.; Novaro, O.; López, T.; Gómez, R. *J. Phys. Chem. B* **1999**, *103*, 299.
(30) Liu, P.; Skogsmo, J. *Acta Crystallogr. B* **1991**, *47*, 425.
(31) Wilson, S. J.; Stacey, M. H. J. *J. Colloid Interface Sci.* **1981**, *82*, 507.
(32) Soled, S. J. *Catalysis* **1983**, *81*, 252.